# Anion and Cation Dynamics in Mixed-Anion Hydroborate Na3(BH4)(B12H12): 1H, 11B, and 23Na NMR Studies

Olga A. Babanova , Yolanda Sadikin , Roman V. Skoryunov , Alexei V. Soloninin , Alexander V. Skripov *

Posted Date: 9 August 2024

doi: 10.20944/preprints202408.0715.v1

Keywords: hydroborates; reorientations; diffusion; nuclear magnetic resonance

*Article*

# Anion and Cation Dynamics in Mixed-Anion Hydroborate $Na_3(BH_4)(B_{12}H_{12})$: $^{1}H$, $^{11}B$, and $^{23}Na$ NMR Studies

**Olga A. Babanova [1], Yolanda Sadikin [2], Roman V. Skoryunov [1], Alexei V. Soloninin [1] and Alexander V. Skripov [1,*]**

[1] Institute of Metal Physics, Ural Division of the Russian Academy of Sciences, S. Kovalevskoi 18, Ekaterinburg 620108, Russia
[2] Laboratory of Crystallography, Department of Quantum Matter Physics, University of Geneva, Quai Ernest-Ansermet 24, 1211 Geneva, Switzerland
* Correspondence: skripov@imp.uran.ru

**Abstract:** Sodium borohydride-*closo*-hydroborate $Na_3(BH_4)(B_{12}H_{12})$ exhibits the high room-temperature ionic conductivity and high electrochemical stability. To study the dynamical properties of this mixed-anion compound at the microscopic level, we have measured the $^{1}H$, $^{11}B$, and $^{23}Na$ nuclear magnetic resonance spectra and nuclear spin-lattice relaxation rates over the temperature range of 8 – 573 K. Our $^{1}H$ and $^{11}B$ spin-lattice relaxation measurements have revealed two types of reorientational jump motion. The faster motional process attributed to reorientations of the $[BH_4]^-$ anions is characterized by the activation energy of 159 meV, and the corresponding reorientational jump rate reaches ~$10^8$ $s^{-1}$ near 130 K. The slower process ascribed to reorientations of the larger $[B_{12}H_{12}]^{2-}$ anions is characterized by the activation energy of 319 meV, and the corresponding reorientational jump rate reaches ~$10^8$ $s^{-1}$ near 240 K. The results of the $^{23}Na$ nuclear magnetic resonance measurements are consistent with the fast long-range diffusion of $Na^+$ ions in $Na_3(BH_4)(B_{12}H_{12})$. The diffusive jump rate of $Na^+$ is found to reach ~$10^4$ $s^{-1}$ at 300 K and ~$8 \times 10^8$ $s^{-1}$ at 530 K. Comparison of these jump rates with the ionic conductivity data suggests the importance of correlations between diffusing ions.

**Keywords:** hydroborates; reorientations; diffusion; nuclear magnetic resonance

## 1. Introduction

Metal hydroborates are a fascinating class of materials that exhibit remarkably diverse structural chemistries and properties [1,2]. The discovery of superionic conductivity in alkali-metal borohydrides [3] and *closo*-borates [4,5] has attracted additional interest to these materials as prospective solid electrolytes for batteries [6–8]. It should be noted that high ionic conductivities are usually observed above the order-disorder phase transition points, while the ordered (low-temperature) phases of both borohydrides and *closo*-borates exhibit poor ionic conductivities. Since the order-disorder phase transitions in these compounds typically occur above room temperature, for practical applications, it would be desirable to reduce the phase transition point and to retain the disordered phase down to lower temperatures. One of the possible strategies for stabilizing the disordered phase is based on anion mixing. This strategy has proved to be effective both for borohydrides (where $[BH_4]^-$ anions are partially replaced by halide anions [9,10]) and for *closo*-borates (where nearly spherical $[B_{12}H_{12}]^{2-}$ or $[CB_{11}H_{12}]^-$ anions are partially substituted by ellipsoid-shaped $[B_{10}H_{10}]^{2-}$ or $[CB_9H_{10}]^-$ [11–14]). Recently, the mixed-anion borohydride – *closo*-hydroborate compounds $Na_3(BH_4)(B_{12}H_{12})$, $(Li_{0.7}Na_{0.3})_3(BH_4)(B_{12}H_{12})$, and $K_3(BH_4)(B_{12}H_{12})$ have been synthesized using mechanochemistry methods [15,16]. $Na_3(BH_4)(B_{12}H_{12})$ is found to retain the same structure in a wide temperature range of 100 – 653 K showing rather high ionic conductivity of $0.5 \times 10^{-3}$ S/cm at

 doi:10.20944/preprints202408.0715.v1



room temperature [15]. In contrast, $K_3(BH_4)(B_{12}H_{12})$ exhibits two structural phase transitions at high temperatures (at ~565 K and ~680 K) and the low ionic conductivity of $2\times10^{-6}$ S/cm at 380 K [16].

The important dynamical feature of metal hydroborates is that the complex anions can participate in the fast reorientational (rotational) motion [17]. This motion strongly contributes to the balance of energies determining the thermodynamic stability of hydroborates. Furthermore, the reorientational motion of complex anions may play a significant role in the ionic conductivity mechanisms, facilitating fast cation diffusion [18–21]. In the present work, we use $^{1}$H, $^{11}$B, and $^{23}$Na nuclear magnetic resonance (NMR) measurements of the spectra and nuclear spin-lattice relaxation rates to obtain microscopic information on both the reorientational motion of complex anions ($[BH_4]^-$ and $[B_{12}H_{12}]^{2-}$) and the diffusive motion of $Na^+$ cations in the mixed-anion hydroborate $Na_3(BH_4)(B_{12}H_{12})$. The results will be compared to those for the previously investigated mixed-anion compound $K_3(BH_4)(B_{12}H_{12})$ [16].

## 2. Materials and Methods

The synthesis of $Na_3(BH_4)(B_{12}H_{12})$ was analogous to that described in Ref. [15]. The mixed-anion compound was prepared by ball-milling the 1:1 mixture of $NaBH_4$ (from Sigma-Aldrich) and $Na_2B_{12}H_{12}$ (from Katchem) and consecutive heat treatment to 673 K in aluminum crucible in a closed system at the rate of 5 K/min. All sample handling was done in a glovebox under argon atmosphere. According to X-ray powder diffraction analysis [15], $Na_3(BH_4)(B_{12}H_{12})$ retains the orthorhombic crystal structure (space group $Cmc2_1$) in the temperature range of 100 – 653 K with the lattice parameters $a$ = 8.0083(4) Å, $b$ = 21.881(1) Å, and $c$ = 7.7672(4) Å at 523 K. The schematic view of this structure is shown in Figure 1.

For NMR experiments, the sample was flame-sealed in a quartz tube under vacuum. Low-field NMR measurements of the spectra and spin-lattice relaxation rates were performed on a pulse spectrometer with quadrature phase detection at the frequencies $\omega/2\pi$ = 14 and 28 MHz ($^{1}$H), 28 MHz ($^{11}$B) and 23 MHz ($^{23}$Na). The magnetic field was provided by a 2.1 T iron-core Bruker magnet. A home-built multinuclear continuous-wave NMR magnetometer working in the range 0.32 – 2.15 T was used for field stabilization. For rf pulse generation, we used a SpinCore PB24-100-4K computer-controlled pulse programmer, the PTS frequency synthesizer (Programmed Test Sources, Inc.), and a 1 kW Kalmus wideband pulse amplifier. Typical values of the $\pi/2$ pulse length were 2 – 3 μs for $^{1}$H and 3 – 4 μs for $^{11}$B and $^{23}$Na. A probe head with the sample was placed into an Oxford Instruments CF1200 continuous-flow cryostat using nitrogen or helium as a cooling agent. The sample temperature, monitored by a chromel-(Au-Fe) thermocouple, was stable to ±0.1 K. Measurements at $T$ > 450 K were performed using a furnace probe head; for this setup, the sample temperature, monitored by a copper – constantan thermocouple, was stable to ±0.5 K. High-field measurements of the $^{23}$Na spin-lattice lattice relaxation rate were performed on a Bruker AVANCE III 500 spectrometer at the frequency $\omega/2\pi$ = 132 MHz. The nuclear spin-lattice relaxation rates were measured using the saturation–recovery method. NMR spectra were recorded by Fourier transforming the solid echo signals (pulse sequence $\pi/2_x - t - \pi/2_y$).

 doi:10.20944/preprints202408.0715.v1



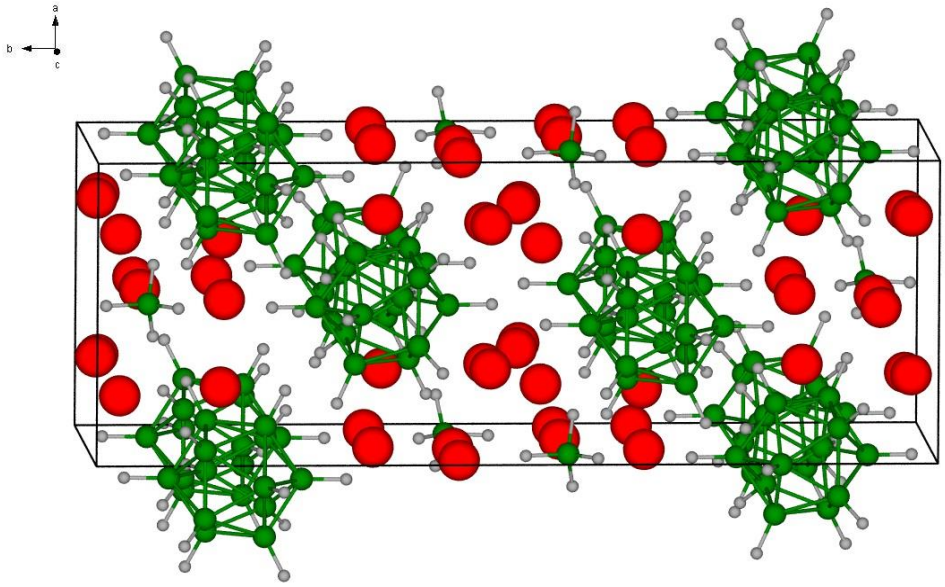


**Figure 1.** Schematic view of the crystal structure of $Na_3(BH_4)(B_{12}H_{12})$ on the basis of X-ray powder diffraction data at 523 K [15]. Red spheres: partially occupied Na sites; green spheres: B atoms; gray spheres: H atoms.

## 3. Results and Discussion

**$^1$H and $^{11}$B nuclear magnetic resonance results.** The evolution of the $^1$H NMR spectra for $Na_3(BH_4)(B_{12}H_{12})$ with temperature is shown in Figure 2. The spectra exhibit a considerable narrowing with increasing temperature, which can be attributed to a partial averaging of dipole-dipole interactions of $^1$H spins due to jump motion of H atoms. Figure 3 shows the temperature dependence of the $^1$H line width $\Delta_H$ (full width at half-maximum). It should be noted that at high temperatures, $\Delta_H$ does not drop to very small values, remaining on a plateau of approximately 10 kHz. This feature (typical of all the studied hydroborates [17,19,22]) indicates the *localized* nature of the motion of H atoms, as can be expected for anion reorientations. In contrast to the long-range translational diffusion, the localized motion leads to only partial averaging of the dipole-dipole interactions between moving nuclear spins.

 doi:10.20944/preprints202408.0715.v1



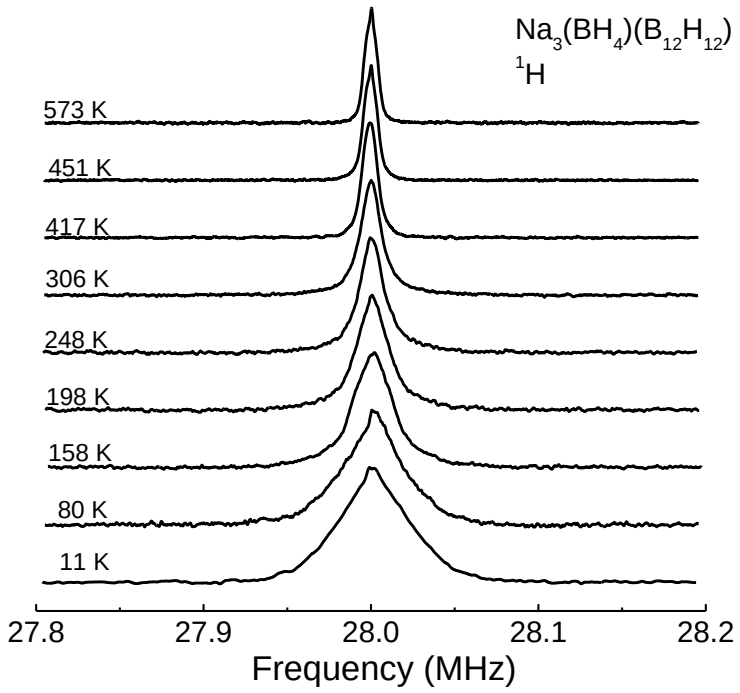


**Figure 2.** Evolution of the $^{1}$H NMR spectra for $Na_3(BH_4)(B_{12}H_{12})$ with temperature.

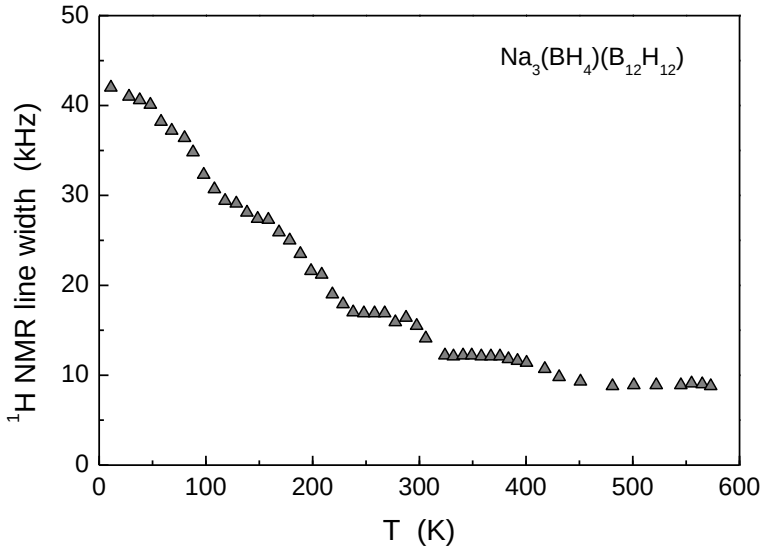


**Figure 3.** Temperature dependence of the width (full width at half-maximum) of the $^{1}$H NMR spectra measured at 28 MHz for $Na_3(BH_4)(B_{12}H_{12})$.

Quantitative information on the H jump rates $\tau^{-1}$ can be obtained from measurements of the $^{1}$H spin-lattice relaxation rate $R_1^H$. Figure 4 shows the measured $^{1}$H spin-lattice relaxation rates at two resonance frequencies $\omega/2\pi$ as functions of the inverse temperature. As can be seen from this figure, $R_1^H(T)$ exhibits two frequency-dependent peaks near 240 K and 130 K. Such $R_1^H(T)$ peaks

 doi:10.20944/preprints202408.0715.v1



are typical of many hydroborate systems [17,19,22]; they occur at the temperatures, at which the jump rates $\tau^{-1}$ of anion reorientations become approximately equal to the resonance frequency $\omega$ (~$10^8$ $s^{-1}$). The observation of two $R_1^H(T)$ maxima indicates a coexistence of two types of reorientational motion with different characteristic rates, as can be expected in the case of two types of the anions.

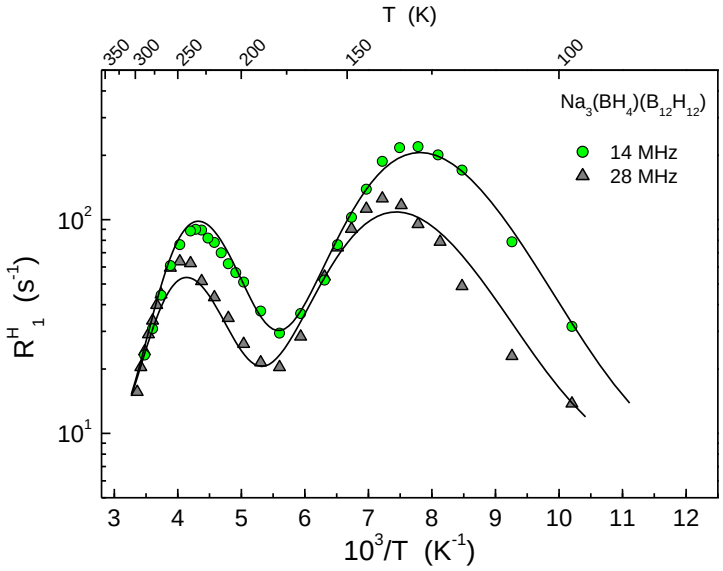


**Figure 4.** Proton spin-lattice relaxation rates measured at 14 and 28 MHz for $Na_3(BH_4)(B_{12}H_{12})$ as functions of the inverse temperature. The solid curves show the simultaneous fit of the two-peak model with Gaussian distributions of the activation energies in the temperature range of 98 – 298 K.

To distinguish between reorientations of the $[BH_4]^-$ and $[B_{12}H_{12}]^{2-}$ anions, we have used the behavior of the $^{11}B$ spin-lattice relaxation rate $R_1^B$. For $R_1^B(T)$, we may also expect the peaks related to the reorientational motion; however, the amplitudes of these peaks should differ significantly. The amplitude of the $R_1^B(T)$ peak due to $B_{12}H_{12}$ reorientations is determined by strong fluctuations of the electric quadrupole interaction of $^{11}B$ nuclei [22]. This amplitude should be considerably higher than the amplitude of the $R_1^B(T)$ peak due to $BH_4$ reorientations, since for the latter the quadrupole interaction is relatively unimportant, because of the special position of B atom in the center of the nearly regular tetrahedron. Indeed, a reorientational jump of $BH_4$ tetrahedron does not change a configuration of H atoms surrounding B atom, and the electric field gradient at B site remains nearly the same. The difference between the amplitudes of the $R_1^B(T)$ peaks due to $B_{12}H_{12}$ and $BH_4$ reorientations is consistent with the experimental results for *closo*-borates and borohydrides [17,22,23].

The results of the $^{11}B$ spin-lattice relaxation measurements for $Na_3(BH_4)(B_{12}H_{12})$ are shown in Figure 5. It should be noted that at $T < 200$ K the recovery of the $^{11}B$ nuclear magnetization deviates from a single-exponential behavior. As in the case of $K_3(BH_4)(B_{12}H_{12})$ [16], such deviations may be related to nonzero electric quadrupole moment of $^{11}B$ nuclei [24] and to the presence of several well-separated inequivalent $^{11}B$ nuclei relaxing with different rates. The relaxation curves at $T < 200$ K can be satisfactorily approximated by sums of two exponential components. The $^{11}B$ spin-lattice relaxation rates shown in Figure 5 correspond to the single exponent at $T > 200$ K and to the faster (dominant) exponential component at $T < 200$ K.

 doi:10.20944/preprints202408.0715.v1



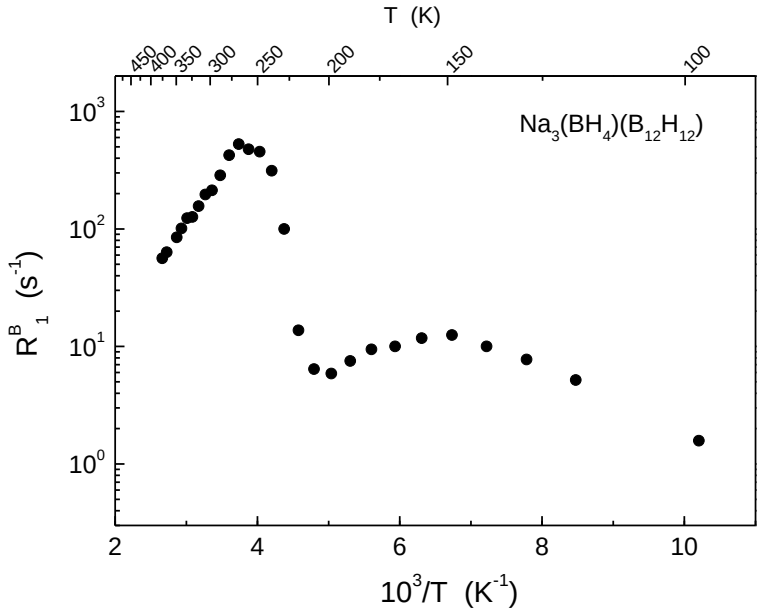


**Figure 5.** $^{11}$B spin-lattice relaxation rates measured at 28 MHz as functions of the inverse temperature. At $T$ > 200 K, the data points represent the results of a single-exponential approximation of the $^{11}$B longitudinal relaxation, and at $T$ < 200 K, they represent the faster component of the two-exponential relaxation.

As can be seen from Figure 5, $R_1^B(T)$ exhibits two peaks in the same temperature ranges as the corresponding $R_1^H(T)$ peaks. On the basis of the observed amplitudes of the $R_1^B(T)$ peaks, we can conclude that the low-temperature peak originates from $BH_4$ reorientations, and the high-temperature one is due to $B_{12}H_{12}$ reorientations. Note that the $^1$H and $^{11}$B relaxation results resemble those found for $K_3(BH_4)(B_{12}H_{12})$ [16]; however, the relaxation-rate peaks for the Na-based system (near 240 K and near 130 K) are shifted to considerably lower temperatures with respect to those for the K-based system (near 390 K and near 200 K, respectively [16]). These results indicate higher reorientational mobility of both $[BH_4]^-$ and $[B_{12}H_{12}]^{2-}$ anions in the Na-based compound. Such a difference may be related to the smaller size of $Na^+$ cations.

For parametrization of the proton spin-lattice relaxation data, we have used the model based on two independent reorientational processes with the H jump rates $\tau_i^{-1}$ ($i$ = 1, 2). Similar model have been previously employed for $K_3(BH_4)(B_{12}H_{12})$ [16]. We assume that $i$ = 1 corresponds to the faster process. According to the standard theory of nuclear spin-lattice relaxation due to the motionally-modulated dipole-dipole interaction [25], in the limit of slow motion ($\omega\tau_i \gg 1$), $R_{1i}^H$ is proportional to $\omega^{-2}\tau_i^{-1}$, and in the limit of fast motion ($\omega\tau_i \ll 1$), $R_{1i}^H$ is proportional to $\tau_i$, being frequency-independent. If the temperature dependence of both H jump rates follows the Arrhenius law,

$$\tau_i^{-1} = \tau_{0i}^{-1} \exp(-E_{ai}/k_BT) \qquad (1)$$

with the activation energy $E_{ai}$ for the $i$th type of motion, for each of the peaks, the plot of $\ln R_{1i}^H$ vs. $T^{-1}$ is expected to be linear in the limits of both slow and fast motion with the slopes of $-E_{ai}/k_B$ and $E_{ai}/k_B$, respectively. The behavior of the proton spin-lattice relaxation rate shown in Figure 4 exhibits some deviations from the predictions of the standard theory. First, for both relaxation rate peaks, the high-$T$ slope appears to be steeper than the low-$T$ one. Second, at the low-$T$ slope of each of the peaks, the frequency dependence of $R_{1i}^H$ is weaker than the predicted $\omega^{-2}$ dependence. These features suggest the presence of a certain distribution of the H jump rates [26]. The simplest approach to introducing

 doi:10.20944/preprints202408.0715.v1



such a distribution is based on using a Gaussian distribution of the activation energies [26]. The details of the two-peak model [27] used for analysis of the proton spin-lattice relaxation data for $Na_3(BH_4)(B_{12}H_{12})$ are presented in the Supplementary Information. The model parameters are the average activation energies $\overline{E}_{ai}$, the distribution widths (dispersions) $\Delta E_{ai}$, the pre-exponential factors $\tau_{0i}$, and the amplitude factors $\Delta M_i$ determined by the strength of the fluctuating part of dipole-dipole interaction between nuclear spins for the $i$th type of motion. These parameters have been varied to find the best fit of the model to the experimental $R_1^H(T)$ data at two resonance frequencies *simultaneously*. The results of this simultaneous fit over the temperature range of 98 – 298 K are shown by black solid curves in Figure 4; the corresponding parameters are $\overline{E}_{a1}$ = 159(5) meV, $\Delta E_{a1}$ = 14(2) meV, $\tau_{01} = 5.9(3) \times 10^{-15}$ s, $\Delta M_1 = 8.2(2) \times 10^9$ s$^{-2}$ (for the faster process of $BH_4$ reorientations), and $\overline{E}_{a2}$ = 319(4) meV, $\Delta E_{a2}$ = 26(3) meV, $\tau_{02} = 1.2(2) \times 10^{-15}$ s, $\Delta M_2 = 3.8(2) \times 10^9$ s$^{-2}$ (for the slower process of $B_{12}H_{12}$ reorientations). Comparison of these results with those obtained for $K_3(BH_4)(B_{12}H_{12})$ [16] indicates that the average activation energies for both reorientational processes in $Na_3(BH_4)(B_{12}H_{12})$ are considerably lower than the corresponding activation energies in $K_3(BH_4)(B_{12}H_{12})$ (236 meV for $BH_4$ reorientations and 594 meV for $B_{12}H_{12}$ reorientations [16]). This is consistent with the higher reorientational mobility of both anions in $Na_3(BH_4)(B_{12}H_{12})$.

**$^{23}$Na nuclear magnetic resonance results.** Information on the cation ($Na^+$) dynamics can be obtained from $^{23}$Na NMR measurements. The $^{23}$Na NMR spectra have been studied in the low magnetic field (at the resonance frequency of 23 MHz) over a wide temperature range (8 – 552 K). The $^{23}$Na spin-lattice relaxation rate measurements (which require better signal-to-noise ratios) have been performed in the high field (at the resonance frequency of 132 MHz) above room temperature. Representative shapes of the $^{23}$Na NMR spectra at three temperatures are shown in Figure S1 of the Supplementary Information. Figure 6 shows the temperature dependence of the $^{23}$Na NMR line width $\Delta_{Na}$ (full width at half-maximum).

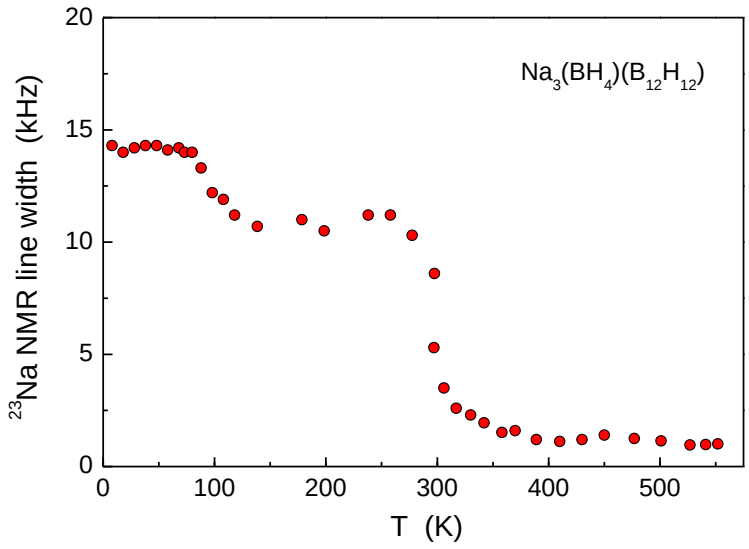


**Figure 6.** Temperature dependence of the $^{23}$Na NMR line width (full width at half-maximum) measured at 23 MHz.

As the temperature increases, the line width becomes smaller due to motional averaging of the local magnetic and electric fields at Na sites. As can be seen from Figure 6, the temperature

 doi:10.20944/preprints202408.0715.v1



dependence of $\Delta_{Na}$ exhibits two characteristic "steps". The minor "step" near 100 K can be ascribed to the excitation of the reorientational motion of $BH_4$ groups inducing fluctuations of the $^1H$ – $^{23}Na$ dipole-dipole interaction. The major "step" near 300 K can be attributed to diffusive motion of $Na^+$ cations themselves, since this motion averages out all dipole-dipole and quadrupole interactions of $^{23}Na$ nuclei. Indeed, in contrast to the case of $\Delta_H$, the $^{23}Na$ line width at high temperatures is very small (~ 1 kHz), which indicates that $Na^+$ cations participate in the *long-range* diffusion. At the temperature of the main "step", the diffusive jump rate $\tau_d^{-1}$ is expected [25] to become nearly equal to the "rigid lattice" line width (~ $10^4$ $s^{-1}$).

To probe the diffusive motion in the range of higher jump rates, we can use the $^{23}Na$ spin-lattice relaxation measurements, since for these measurements, the characteristic frequency scale is determined by the resonance frequency $\omega$ (~ $10^8$ – $10^9$ $s^{-1}$). Figure 7 shows the measured $^{23}Na$ spin-lattice relaxation rate $R_1^{Na}$ as a function of the inverse temperature.

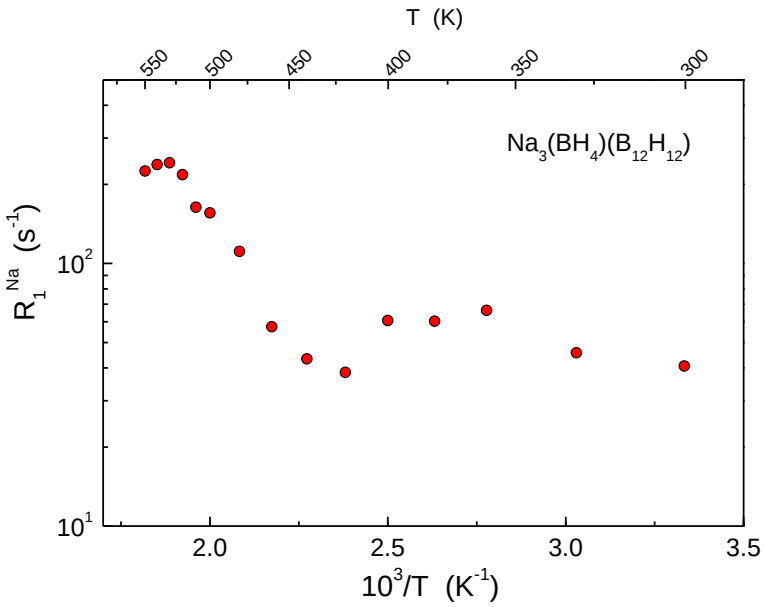


**Figure 7.** $^{23}Na$ spin-lattice relaxation rate measured at 132 MHz as a function of the inverse temperature.

As can be seen from this figure, above 420 K, $R_1^{Na}(T)$ exhibits a significant increase, reaching a maximum near 530 K. The measured $R_1^{Na}$ values in the region of the maximum are much higher than those expected for the $^{23}Na$ – $^1H$ dipole-dipole interaction; therefore, the $^{23}Na$ spin-lattice relaxation is dominated by fluctuations of the quadrupole interaction resulting from $Na^+$ jumps. This is a typical feature of all the studied sodium hydroborates [5,17,22]. At the temperature of the $R_1^{Na}(T)$ maximum, the $Na^+$ jump rate is expected to be nearly equal to the resonance frequency, i. e., $\tau_d^{-1}$ (530 K) ≈ 8 × $10^8$ $s^{-1}$. The activation energy for $Na^+$ diffusion estimated from the slope of the $R_1^{Na}(T)$ peak is 390 meV. For comparison, the activation energy derived from the ionic conductivity data in the range of 273 – 468 K is 340 meV [15].

Possible diffusion pathways were analyzed on the basis of the structure of $Na_3(BH_4)(B_{12}H_{12})$ [15]. According to this analysis, $Na^+$ cations jump between the tetrahedral interstitial sites forming layers perpendicular to the *b* axis, i. e., the diffusion is expected to be quasi-two-dimensional [15]. The distance between the nearest-neighbor Na sites is approximately 2.30 Å. Neglecting any correlations

 doi:10.20944/preprints202408.0715.v1



in diffusive jump motion, the tracer diffusion coefficient of $Na^+$ ions for the case of two-dimensional diffusion can be estimated as $D = L^2/4\tau_d$, where $L$ is the elementary jump length. Taking the distance between the nearest-neighbor Na sites as an estimate of $L$, and using $\tau_d$ at the temperature of the $R_1^{Na}(T)$ maximum, we obtain $D$(530 K) ≈ 1.1 × $10^{-7}$ $cm^2/s$. This value is close to that found from the direct pulsed-field-gradient (PFG) NMR measurements of $Li^+$ diffusivity in $LiLa(BH_4)_3Cl$ ($D$(403 K) = 1.13 × $10^{-7}$ $cm^2/s$ [28]). However, the estimated diffusivity in $Na_3(BH_4)(B_{12}H_{12})$ at 530 K is much lower than the record $Na^+$ diffusivity found from the PFG-NMR measurements for the mixed-anion $Na_2(CB_9H_{10})(CB_{11}H_{12})$ ($D$(403 K) = 8.7 × $10^{-6}$ $cm^2/s$ [29]).

Following Matsuo et al. [3], for comparison of the NMR diffusivity data with the ionic conductivity $\sigma$, we can use the Nernst-Einstein equation,

$$\sigma = nD(Ze)^2/k_BT \quad (2)$$

where $n$ is the number of charge carriers per unit volume, and $Ze$ is the electrical charge of the carrier. It should be noted that this equation assumes uncorrelated diffusion. Using the above estimate of $D$(530 K) and the value of $n$ = 8.8 × $10^{21}$ $cm^{-3}$ found on the basis of the structural data [15], we obtain from Eq. (2) that $\sigma$(530 K) = 4.3 × $10^{-3}$ S/cm. Experimentally, the ionic conductivity was measured up to 473 K, and its value at this temperature was 1.5 × $10^{-2}$ S/cm [15]. Taking into account the Arrhenius-type behavior of the measured $\sigma$ [15], its extrapolation to 530 K gives $\sigma_{ext}$(530 K) = 5.0 × $10^{-2}$ S/cm. Thus, the ionic conductivity estimated from the NMR diffusivity data appears to be nearly an order of magnitude lower than the corresponding experimental (extrapolated) value. Similar situation has been well documented in the case of the mixed-anion $Li(CB_9H_{10})_{0.7}(CB_{11}H_{12})_{0.3}$ system [7] and the disordered $LiCB_9H_{10}$ phase [28], where the measured conductivities are considerably higher than those derived from the PFG-NMR diffusivity data on the basis of the Nernst-Einstein equation. Such effects have been attributed to strong correlations between the diffusing ions (concerted diffusion) [30–32].

## 4. Conclusions

The results of our $^1H$ and $^{11}B$ spin-lattice relaxation measurements have revealed two types of reorientational jump motion in the mixed-anion hydroborate $Na_3(BH_4)(B_{12}H_{12})$. The faster motional process is assigned to reorientations of the $[BH_4]^-$ anions. This process is characterized by the activation energy of 159(5) meV, and the corresponding reorientational jump rate reaches ~$10^8$ $s^{-1}$ near 130 K. The slower process attributed to reorientations of the larger $[B_{12}H_{12}]^-$ anions is characterized by the activation energy of 319(4) meV, and the corresponding reorientational jump rate reaches ~$10^8$ $s^{-1}$ near 240 K. Comparison of these results with those obtained for the related mixed-anion hydroborate $K_3(BH_4)(B_{12}H_{12})$ with rather low ionic conductivity [16] shows that the reorientational mobilities of both anions in the Na-based compound are considerably higher than the corresponding mobilities in the K-based counterpart. Such a comparison supports the idea that anion reorientations may facilitate the cation diffusion.

The results of the $^{23}Na$ NMR measurements are consistent with the fast long-range diffusion of $Na^+$ ions in $Na_3(BH_4)(B_{12}H_{12})$. The diffusive jump rate is found to reach ~$10^4$ $s^{-1}$ at 300 K and ~8 × $10^8$ $s^{-1}$ at 530 K. The tracer diffusion coefficient of Na-ions estimated at 530 K is 1.1 × $10^{-7}$ $cm^2/s$. However, this diffusivity appears to be nearly an order of magnitude lower than that estimated from the measured ionic conductivity [16] on the basis of the Nernst-Einstein relation; this may be attributed to strong correlations between diffusing ions.

**Supplementary Materials:** The following supporting information can be downloaded at the website of this paper posted on Preprints.org. Expressions used for analysis of the proton spin-lattice relaxation rates, Figure S1: Representative shapes of the $^{23}Na$ NMR spectra at 8 K, 198 K, and 552 K.

**Author Contributions:** O. A. B.: Investigation, Software, Formal Analysis, Writing – original draft; Y. S.: Synthesis and Characterization; R. V. S.: Investigation, Visualization; A. V. S. (Alexei V. Soloninin): Investigation, Methodology, Validation; A. V. S. (Alexander V. Skripov): Supervision, Writing – review and editing. All the authors have read and agreed to the final version of the manuscript.

**Funding:** This work was performed within the assignment of the scientific program "Function" (No. 122021000035-6) of the Ural Branch of the Russian Academy of Sciences.

**Acknowledgments:** The authors are grateful to R. Černý for useful discussions.

**Data Availability:** Data are available on request from the authors.

**Conflicts of Interest**: The authors declare no conflicts of interest.

## References

1. Paskevicius, M.; Jepsen, L.; Schouwink, P.; Černý, R.; Ravnsbæk, D.B.; Filinchuk, Y.; Dornheim, M.; Besenbacher, F.; Jensen, T.R. Metal Borohydrides and Derivatives – Synthesis, Structure and Properties. *Chem.Soc. Rev.* **2017**, *46*, 1565-1634.
2. Černý, R.; Brighi, M.; Murgia, F. The Crystal Chemistry of Inorganic Hydroborates. *Chemistry* **2020**, *2*, 805-826.
3. Matsuo, M.; Nakamori, Y.; Orimo, S.; Maekawa, H.; Takamura H. Lithium Superionic Conduction in Lithium Borohydride Accompanied by Structural Transition. *Appl. Phys. Lett.* **2007**, *91*, 224103.
4. Udovic, T.J.; Matsuo, M.; Unemoto, A.; Verdal, N.; Stavila, V.; Skripov, A.V.; Rush, J.J.; Takamura, H.; Orimo, S. Sodium Superionic Conduction in $Na_2B_{12}H_{12}$. *Chem. Commun.* **2014**, *50*, 3750-3752.
5. Tang, W.S.; Matsuo, M.; Wu, H.; Stavila, V.; Zhou, W.; Talin, A.A.; Soloninin, A.V.; Skoryunov, R.V.; Babanova O.A.; Skripov, A.V.; Unemoto, A.; Orimo, S.; Udovic T.J. Liquid-like Ionic Conduction in Solid Lithium and Sodium Monocarba-*Closo*-Decaborates Near or at Room Temperature. *Adv. Energy Mater.* **2016**, *6*, 1502237.
6. Yoshida, K.; Sato, T.; Unemoto, A.; Matsuo, M.; Ikeshoji, T.; Udovic, T.J.; Orimo, S. Fast Sodium Ionic Conduction in $Na_2B_{10}H_{10}$-$Na_2B_{12}H_{12}$ Complex Hydride and Application to a Bulk-Type All-Solid-State Battery. *Appl. Phys. Lett.* **2017**, *110*, 103901.
7. Kim, S.; Oguchi, H.; Toyama, N.; Sato, T.; Takagi, S.; Otomo, T.; Arunkumar, D.; Kuwata, N.; Kawamura, J.; Orimo, S. A Complex Hydride Lithium Superionic Conductor for High-Energy-Density All-Solid-State Lithium Metal Batteries. *Nat. Commun.* **2019**, *10*, 1081.
8. Duchêne, L.; Remhof, A.; Hagemann, H.; Battaglia, C. Status and Prospects of Hydroborate Electrolytes for All-Solid-State Batteries. *Energy Storage Mater.* **2020**, *25*, 782-794.
9. Maekawa, H.; Matsuo, M.; Takamura, H.; Ando, M.; Noda, Y.; Karahashi, T.; Orimo, S. Halide-Stabilized $LiBH_4$, A Room-Temperature Lithium Fast-Ion Conductor. *J. Am. Chem. Soc.* **2009**, *131*, 894-895.
10. Rude, L.H.; Groppo, E.; Ambjerg, L.M.; Ravnsbæk, D.B.; Malmkjær, M.A.; Filinchuk, Y.; Baricco, M.; Besenbacher, F.; Jensen, T.R. Iodide Substitution in Lithium Borohydride, $LiBH_4$ – LiI. *J. Alloys Compd.* **2011**, *509*, 8299-8305.
11. Tang, W.S.; Yoshida, K.; Soloninin, A.V.; Skoryunov, R.V.; Babanova, O.A.; Skripov, A.V.; Dimitrievska, M.; Stavila, V.; Orimo, S.; Udovic, T.J. Stabilizing Superionic-Conducting Structures via Mixed-Anion Solid Solutions of Monocarba-*Closo*-Borate Salts. *ACS Energy Lett.* **2016**, *1*, 659-664.
12. Duchêne, L.; Kühnel, R.-S.; Rentsch, D.; Remhof, A.; Hagemann, H.; Battaglia, C. A Highly Stable Sodium Solid-State Electrolyte Based on a Dodeca/Deca-Borate Equimolar Mixture. *Chem. Commun.* **2017**, *53*, 4195-4198.
13. Brighi, M.; Murgia, F.; Łodziana, Z.; Schouwink, P.; Wołczyk, A.; Černý, R. A Mixed Anion Hydroborate/Carba-Hydroborate as a Room Temperature Na-Ion Solid Electrolyte. *J. Power Sources*, **2018**, *404*, 7-12.
14. Brighi, M.; Murgia, F.; Černý, R. *Closo*-Hydroborate Sodium Salts as an Emerging Class of Room-Temperature Solid Electrolytes. *Cell Rep. Phys. Sci.* **2020**, *1*, 100217.
15. Sadikin, Y.; Brighi, M.; Schouwink, P.; Černý, R. Superionic Conduction of Sodium and Lithium in Anion-Mixed Hydroborates $Na_3BH_4B_{12}H_{12}$ and $(Li_{0.7}Na_{0.3})_3BH_4B_{12}H_{12}$. *Adv. Energy Mater.* **2015**, 1501016.
16. Sadikin, Y.; Skoryunov, R.V.; Babanova, O.A.; Soloninin, A.V.; Łodziana, Z.; Brighi, M.; Skripov, A.V.; Černý, R. Anion Disorder in $K_3BH_4B_{12}H_{12}$ and Its Effect on Cation Mobility. *J. Phys. Chem. C* **2017**, *121*, 5503-5514.
17. Skripov, A.V.; Soloninin, A.V.; Babanova O.A.; Skoryunov, R.V. Anion and Cation Dynamics in Polyhydroborate Salts: NMR Studies. *Molecules* **2020**, *25*, 2940.
18. Skripov, A.V.; Soloninin, A.V.; Ley M.B.; Jensen, T.R.; Filinchuk, Y. Nuclear Magnetic Resonance Study of $BH_4$ Reorientations and Li Diffusion in $LiLa(BH_4)_3Cl$. *J. Phys. Chem. C* **2013**, *117*, 14965-14972.
19. Skripov, A.V.; Soloninin, A.V.; Babanova, O.A.; Skoryunov, R.V. Nuclear Magnetic Resonance Studies of Atomic Motion in Borohydride-Based Materials: Fast Anion Reorientations and Cation Diffusion. *J. Alloys Compd.* **2015**, *645*, S428-S433.
20. Kweon, K.; Varley, J.B.; Shea, P.; Adelstein, N.; Mehta, P.; Heo, T.W.; Udovic, T.J.; Stavila, V.; Wood, B.C. Structural, Chemical, and Dynamical Frustration: Origins of Superionic Conductivity in *Closo*-Borate Solid Electrolytes. *Chem. Mater.* **2017**, *29*, 9142-9153.

21. Dimitrievska, M.; Shea, P.; Kweon, K.E.; Bercx, M.; Varley, J.B.; Tang, W.S.; Skripov, A.V.; Stavila, V.; Udovic, T.J.; Wood, B.C. (2018) Carbon Incorporation and Anion Dynamics as Synergistic Drivers for Ultrafast Diffusion in Superionic $LiCB_{11}H_{12}$ and $NaCB_{11}H_{12}$. *Adv. Energy Mater.* **2018**, *8*, 1703422.
22. Skripov, A.V.; Babanova, O.A.; Soloninin, A.V.; Stavila, V.; Verdal, N.; Udovic, T.J.; Rush, J.J. Nuclear Magnetic Resonance Study of Atomic Motion in $A_2B_{12}H_{12}$ (A = Na, K, Rb, Cs): Anion Reorientations and $Na^+$ Mobility. *J. Phys. Chem. C* **2013**, *117*, 25961-25968.
23. Babanova, O.A.; Soloninin, A.V.; Stepanov, A.P.; Skripov, A.V.; Filinchuk, Y. Structural and Dynamical Properties of $NaBH_4$ and $KBH_4$: NMR and Synchrotron X-Ray Diffraction Studies. *J. Phys. Chem. C* **2010**, *114*, 3712-3718.
24. Kim, C.; Ku, J.; Hwang, S.J.; Bowman, R.C.; Reiter, J.W. Nuclear Magnetic Relaxation Studies of $BH_4$ in Metal Borohydrides. *Bull. Corean Chem. Soc.* **2021**, 1-12.
25. Abragam, A. *The Principles of Nuclear Magnetism*. Clarendon Press: Oxford, 1961.
26. Markert, J.T.; Cotts, E.J.; Cotts, R.M. Hydrogen Diffusion in the Metallic Glass *a*-$Zr_3RhH_{3.5}$. *Phys. Rev. B* **1988**, *37*, 6446-6452.
27. Skripov, A.V., Soloninin, A.V.; Babanova O.A.; Hagemann, H.; Filinchuk, Y. Nuclear Magnetic Resonance Study of Reorientational Motion in $\alpha$-$Mg(BH_4)_2$. *J. Phys. Chem. C* **2010**, *114*, 12370-12374.
28. Skripov, A.V.; Majer, G.; Babanova, O.A.; Skoryunov, R.V.; Soloninin, A.V.; Ley, M.B.; Jensen, T.R.; Orimo, S.; Udovic, T.J. Lithium-Ion Diffusivity in Complex Hydrides: Pulsed-Field-Gradient NMR Studies of $LiLa(BH_4)_3Cl$, $Li_3(NH_2)_2I$ and Li-1-$CB_9H_{10}$. *Solid State Ionics* **2021**, *362*, 115585.
29. Skripov, A.V.; Majer, G.; Babanova, O.A.; Skoryunov, R.V.; Soloninin, A.V.; Dimitrievska, M.; Udovic, T.J. $Na^+$ Diffusivity in Carbon-Substituted *Nido*- and *Closo*-Hydroborate Salts: Pulsed-Field-Gradient NMR Studies of Na-7-$CB_{10}H_{13}$ and $Na_2(CB_9H_{10})(CB_{11}H_{12})$. *J. Alloys Compd.* **2021**, *850*, 156781.
30. Okazaki, H. Deviation from the Einstein Relation in Average Crystals Self-Diffusion of $Ag^+$ Ions in $\alpha$-$Ag_2S$ and $\alpha$-$Ag_2Se$. *J. Phys. Soc. Jpn.* **1967**, *23*, 355-360.
31. He, X.; Zhu, Y.; Mo, Y. Origin of Fast Ion Diffusion in Super-Ionic Conductors. *Nat. Commun.* **2017**, *8*, 15893.
32. Sau, K.; Takagi, S.; Ikeshoji, T.; Kisu, K.; Sato, R.; dos Santos, E.C.; Li, H.; Mohtadi, R.; Orimo, S. Unlocking the Secrets of Ideal Fast Ion Conductors for All-Solid-State Batteries. *Commun. Mater.* **2024**, *5*, 122.